Journal of Gerontology: BIOLOGICAL SCIENCES
2007, Vol. 62A, No. 7, 696–706

Mechanisms Underlying Hypertrophic Remodeling and Increased Stiffness of Mesenteric Resistance Arteries From Aged Rats

Ana M. Briones,[1,2] Mercedes Salaices,[2] and Elisabet Vila[1]

[1]Departament de Farmacologia, Terapèutica i Toxicología, Facultat de Medicina, Universitat Autònoma de Barcelona and [2]Departamento de Farmacología y Terapéutica, Facultad de Medicina, Universidad Autónoma de Madrid, Spain.

The mechanisms associated with structural and mechanical alterations of mesenteric resistance arteries from aged rats were investigated by using pressure myography, confocal microscopy, immunofluorescence, and picrosirius red staining. Arteries from old rats showed: (i) increased wall and media thickness, greater number of smooth muscle cell (SMC) layers but decreased density of SMC; (ii) increased number of adventitial cells; (iii) hypertrophy of nuclei of SMC and endothelial cells; (iv) increased stiffness associated with increased total collagen content and collagen I/III deposition in the media; and (v) similar content but changes in elastin structure in the internal elastic lamina. Hypertrophic outward remodeling in aged rat resistance arteries involve adventitial cells hyperplasia, reorganization of the same number of hypertrophied SMC in more SMC layers leading to thickened media and endothelial cell hypertrophy. Fibrosis associated with collagen deposition and changes in elastin structure might be responsible for the increased stiffness of resistance arteries from aged rats.

THE process of aging is associated with marked changes in the cardiovascular system that can lead to the development of cardiovascular diseases. With age, the vascular wall of large peripheral arteries undergoes structural changes including stiffness, thickening of the media, and enlargement of the lumen diameter (1–4). However, this process is heterogeneous along the arterial tree (5–7).

Old individuals with increased arterial stiffness and elevated pulse pressure have higher cardiovascular morbidity and mortality (8). Moreover, recent evidence suggests a relationship between pulse pressure and vascular structure in resistance arteries (6,7). In aged rats, mesenteric resistance arteries (MRA) show hypertrophic outward remodeling (i.e., increased lumen size and cross-sectional area [CSA]) associated with stiffness of the wall components (6,7,9). Nevertheless, the processes underlying these changes in resistance arteries remain elusive. In aorta from aged rats, modification in smooth muscle cell (SMC) number, increased collagen deposition, and structural alterations of elastin are characteristic features (3,4). Thus, most studies have found that the number of SMC declines with age (10,11), although unchanged SMC number has also been described (12). Collagen types I and III are increased in conductance arteries with age, and several studies suggest a relative reduction of elastin density (3,4,13). However, an important aspect not well addressed so far in either large or small arteries from aged rats is the possible structural distortion of elastin which might contribute to limit the function of providing capacitance.

The aim of the present study was to investigate the cellular and extracellular matrix (ECM) alterations underlying hypertrophy and increased stiffness of resistance arteries from aged rats. For this purpose, we used confocal microscopy to analyze the putative contribution of each cell type (adventitial, smooth muscle, and endothelial) to the thickened wall of resistance arteries from old rats. Moreover, we have studied changes in collagen and elastin, the most important ECM proteins responsible for vascular elasticity, in resistance vessels from these animals.

Method

Animals

Male Sprague-Dawley rats (Harlan Ibérica, Barcelona, Spain) from 3 to 4 (young) and from 22 to 23 (old) months old were used. The rats were decapitated, and the mesenteric arcade was removed and placed in Krebs–Henseleit solution (KHS) of the following composition (in mM): NaCl 112.0, KCl 4.7, $CaCl_2$ 2.5, KH_2PO_4 1.1, $MgSO_4$ 1.2, $NaHCO_3$ 25.0, and glucose 11.1; maintained at 4°C; and continuously gassed with 95% O_2 and 5% CO_2. A third-order branch of mesenteric artery was isolated from the mesenteric bed and carefully cleaned of surrounding tissue under a dissecting microscope.

Diastolic and systolic blood pressure measurements were taken in rats anesthetized with sodium pentobarbitone (60 mg/Kg, i.p) by means of a Transpack (Abbot, Ireland) transducer connected to a cannula inserted into the right carotid artery. Pulse arterial pressure was taken as the difference between systolic and diastolic pressure. Heart rate was derived from the arterial pulse. Blood pressure and heart rate values used for comparison between age groups were obtained after a 15-minutes stabilization period. The

investigation conforms to the *Guide for the Care and Use of Laboratory Animals* published by the U.S. National Institutes of Health (NIH Publication No. 85-23, revised 1996) and with current Spanish and European laws (RD 223/88 MAPA and 609/86).

Pressure Myography

The structural and mechanical properties of MRA were studied with a pressure myograph (Danish Myo Tech, Model P100; J.P. Trading I/S, Aarhus, Denmark), as previously described (14). Briefly, the vessel was placed on two glass microcannulae and secured with surgical nylon suture. After any small branches were tied off, vessel length was adjusted so that the vessel walls were parallel without stretch. Intraluminal pressure was then raised to 140 mmHg, and the artery was unbuckled by adjusting the cannulae. The segment was then set to a pressure of 70 mmHg and allowed to equilibrate for 60 minutes at 37°C in calcium-free KHS ($0Ca^{2+}$; omitting calcium and adding 10 mM EGTA) gassed with a mixture of 95% O_2 and 5% CO_2. Intraluminal pressure was reduced to 3 mmHg. A pressure-diameter curve was obtained by increasing intraluminal pressure in 20 mmHg steps between 3 and 140 mmHg. Internal and external diameters were continuously measured under passive conditions (D_{i0Ca}, D_{e0Ca}) for 5 minutes at each intraluminal pressure. The final value used was the mean of the measurements taken during the last 30 seconds when the measurements reached a steady state. Finally, the artery was set to 70 mmHg in $0Ca^{2+}$-KHS, pressure-fixed with 4% paraformaldehyde (PFA; in 0.2 M phosphate buffer, pH 7.2–7.4) at 37°C for 60 minutes, and kept in 4% PFA at 4°C for confocal microscopy studies.

Calculation of Structural and Mechanical Parameters

From internal and external diameter measurements in passive conditions, the following structural parameters were calculated:

$$\text{Wall thickness, WT} = (D_{e0Ca} - D_{i0Ca})/2$$
$$\text{CSA} = (\pi/4) \times (D_{e0Ca}{}^2 - D_{i0Ca}{}^2)$$
$$\text{Wall/lumen} = (D_{e0Ca} - D_{i0Ca})/2D_{i0Ca}$$

Luminal surface area (LSA) was calculated at 70 mmHg intraluminal pressure according to the formula:

$$\text{LSA} = 2\,\pi\,L\,(D_{i0Ca}/2),$$

where L is 1 mm length of the vessel.

Incremental distensibility represents the percentage of change of the arterial internal diameter for each mmHg change in intraluminal pressure and was calculated according to the formula:

$$\text{Incremental distensibility} = \Delta D_{i0Ca}/(D_{i0Ca} \times \Delta P) \times 100.$$

Circumferential wall strain (ϵ) = $(D_{i0Ca} - D_{00Ca})/D_{00Ca}$, where D_{00Ca} is the internal diameter at 3 mmHg and D_{i0Ca} is the observed internal diameter for a given intravascular pressure both measured in $0Ca^{2+}$ medium.

Circumferential wall stress (σ) = $(P \times D_{i0Ca})/(2WT)$, where P is the intraluminal pressure (1 mmHg = 1.334×10^3 dynes/cm^2) and WT is measured at each intraluminal pressure in $0Ca^{2+}$ – KHS.

Arterial stiffness independent of geometry is determined by Young's elastic modulus (E = stress/strain). The stress–strain relationship is nonlinear; therefore, it is more appropriate to obtain a tangential or incremental elastic modulus (E_{inc}) by determining the slope of the stress–strain curve ($E_{inc} = \delta\sigma/\delta\varepsilon$) (14). E_{inc} was obtained by fitting the stress–strain data from each animal to an exponential curve using the equation $\sigma = \sigma_{orig}\, e^{\beta\varepsilon}$, where σ_{orig} is the stress at the original diameter (diameter at 3 mmHg). Taking derivatives on the above equation we see that $E_{inc} = \beta\sigma$. For a given σ value, E_{inc} is directly proportional to β. An increase in β implies an increase in E_{inc}, which means an increase in stiffness.

Nuclei Distribution by Confocal Microscopy

Fixed intact arteries were incubated with the nuclear dye, propidium iodide (10 μg/mL). After washing, the arteries were mounted on slides with a well made of silicon spacers to avoid artery deformation. Arteries were viewed using a Leica TCS SP2 AOBS (Leica, Heidelberg, Germany) confocal system fitted with an inverted microscope and argon and helium–neon laser sources with an oil immersion lens (×63) using the 543 nm line of the microscope. Two stacks of images of 0.5 μm-thick serial optical slices were taken from the adventitia to the lumen in different regions along the artery length. Individual images of the endothelial layer were also captured. MetaMorph image analysis software (Universal Imaging Corporation, part of Molecular Devices Corporation, Sunnyvale, CA) was used for quantification of different parameters in the *x*–*y* plane. The adventitia and media thickness and nuclei number were measured in the *z* axis as previously described (15) with minor modifications.

The number of SMC layers in the media was measured in orthogonal reconstructions of the arteries. SMC nuclei were distinguished by their perpendicular orientation in the artery wall. Several measurements were taken in different zones of each artery and averaged.

To allow comparison between young and old rats, the following calculations were performed on the basis of 1 mm-long segments: vessel volume (in mm^3); volume = wall CSA (mm^2) × 1 mm; adventitial and medial volumes (volume = respective layer CSA [mm^2] × 1 mm); total number of cells (adventitial, smooth muscle, or endothelial) (cell *n* = *n* of nuclei per stack × *n* of stacks per vessel volume); LSA = 2πdiameter/2; endothelial cell (EC) density = EC/mm^2 image area; total number of EC was calculated per luminal surface of 1 mm-long vessel, total number EC = EC/mm^2 × LSA.

Elastin Content and Organization by Confocal Microscopy

The content and organization of elastin in MRA were studied in maximally relaxed intact segments pressure-fixed at 70 mmHg by using a confocal microscope as previously described (14). Briefly, serial optical sections (stacks of images) from the adventitia to the lumen (z step = 0.3 μm) were captured with a $\times 63_{oil}$ objective (numeric aperture 1.3)

using the 488 nm line of the confocal microscope. A minimum of two stacks of images of different regions was captured in each arterial segment. All the images were taken under identical conditions of laser intensity, brightness, and contrast.

Quantitative analysis was performed with MetaMorph image analysis software, as described (14). From each stack of serial images, individual projections of the internal elastic lamina (IEL) were reconstructed and IEL thickness, total fenestrae number, fenestra area, and relative area occupied by elastin were measured. Fluorescence intensity values were used as estimates of elastin concentration as previously described (14), based on the assumption that the concentration of elastin has a linear relationship with fluorescence intensity (16).

Collagen Determination by Picrosirius Red

Segments of MRA were removed from the mesentery and immediately fixed in 4% PFA in phosphate buffer for 1 hour, transferred to a cryomold containing OCT embedding medium (Tissue Tek; Sakura, The Netherlands), and frozen in liquid nitrogen. Frozen transverse sections (10 μm) were incubated with picrosirius red (0.1% [wt/vol] sirius red 3FB in saturated aqueous picric acid) for 30 minutes with gentle agitation for collagen staining (17). Color images were captured with a microscope (Nikon Eclipse TE 2000-S, ×40 objective) using a digital camera (Nikon DXM 1200F). Quantitative analysis of collagen content was performed with MetaMorph image analysis software. Original images were transformed to grayscale level. Thereafter, collagen content was estimated by subtracting the background from the intensity values obtained in each cross-section.

Immunofluorescence

For immunofluorescence, third-order branches of the mesenteric artery (~3 mm length) from young and old rats were fixed with 4% phosphate-buffered PFA (in 0.2 M phosphate buffer, pH 7.2–7.4) for 1 hour. Afterwards, arteries were washed in three changes of phosphate-buffered saline (PBS) solution (pH = 7.4). After clearing, arterial segments were placed in PBS containing 30% sucrose. The segments were then transferred to a cryomold containing OCT embedding medium for 20 minutes and frozen in a beaker of isopentane that had been cooled in liquid nitrogen. Tissues were kept at –70°C until the day of the experiments. Frozen transverse sections (14 μm) were cut onto gelatin-coated slides and air-dried for at least 60 minutes. After blockade, sections were incubated with primary monoclonal antibodies against collagen type I/III (1:30; Calbiochem, San Diego, CA) in PBS containing 2% bovine serum albumin for 1 hour at 37°C in a humid box. After washing, rings were incubated with the secondary antibody, a donkey antirabbit immunoglobulin G–conjugated to Cy3 (Jackson ImmunoResearch Laboratories, West Grove, PA) at a dilution of 1:200 for an additional 1 hour at 37°C in a humid box. After washing, immunofluorescent signals were viewed with a confocal microscope (Leica TCS 4D) with a $\times 40_{oil}$ objective. Images of the natural autofluorescence of the elastic components of the arterial wall were also taken. Autofluorescence was visualized by excitation at 488 nm and detection at 490–535 nm. Cy3-labeled antibody was visualized by excitation at 568 nm and detection at 600–700 nm.

The specificity of the immunostaining was evaluated by omission of the primary antibody and processed as above. Under these conditions, no staining was observed in the vessel wall of either young or aged rats.

Statistical Analysis

Results are expressed as mean ± standard error of the mean (*SEM*) and n denotes the number of animals used in each experiment. The dependence of either vascular structure or mechanics on rat strain and intraluminal pressure was studied by a two-way analysis of variance (ANOVA). For specific two means comparisons, Student's t test was used. A value of $p < .05$ was considered significant.

Results

Body weight was greater ($p < .001$) in old (572 ± 10.1 g, $n = 15$) than in young (386.9 ± 5.9 g, $n = 15$) rats. Although changes in diastolic and systolic blood pressure were not statistically different (data not shown), the pulse pressure increased ($p < .05$) with age (old: 33.1 ± 3.3 mmHg; $n = 6$, young: 22.4 ± 0.8 mmHg; $n = 6$). Heart rate was lower ($p < .05$) in old (301 ± 9.2 beats min^{-1}; $n = 6$) than in young (352.7 ± 16.8 beats min^{-1}; $n = 6$) animals.

Vascular Structure and Passive Vascular Mechanics

Figure 1 shows the morphology data of MRA from young and old rats under fully relaxed conditions. Internal and external diameters and CSA were significantly greater in MRA from old compared to young rats (Figure 1). WT was also greater in vessels from old than young rats (young: 44.3 ± 1.4; old: 50.1 ± 2.0 μm; $p < .05$). Aging had no influence in the media/lumen ratio of vessels (data not shown).

Increasing intravascular pressure increased media stress with no significant difference among groups (Figure 2A). Incremental distensibility was similar in mesenteric arteries from both age groups, although at 60 mmHg this parameter decreased in old rats (Figure 2B). MRA from old animals showed a decreased elasticity as shown by the larger value of β (young: 4.03 ± 0.12; old: 4.47 ± 0.15, $p < .05$) and a leftward shift of the stress–strain relationship (Figure 2C).

Morphology of the Vascular Wall

Media and WT were greater in vessels from old than young rats (Figure 3, A and B). However, adventitia thickness remained unaffected by age (Figure 3A). The number of SMC layers was significantly greater in MRA from old than from young rats (young: 3.75 ± 0.14; old: 4.63 ± 0.2, $p < .05$).

Total number of adventitial but not SMC was greater in old than in young rats (Figure 3C). Density of cells in the adventitia remained similar in both age groups, whereas in the media, density of SMC decreased by age (Figure 3D).

As expected, LSA increased with age (Table 1). Total number of EC in the luminal surface was equal in young and

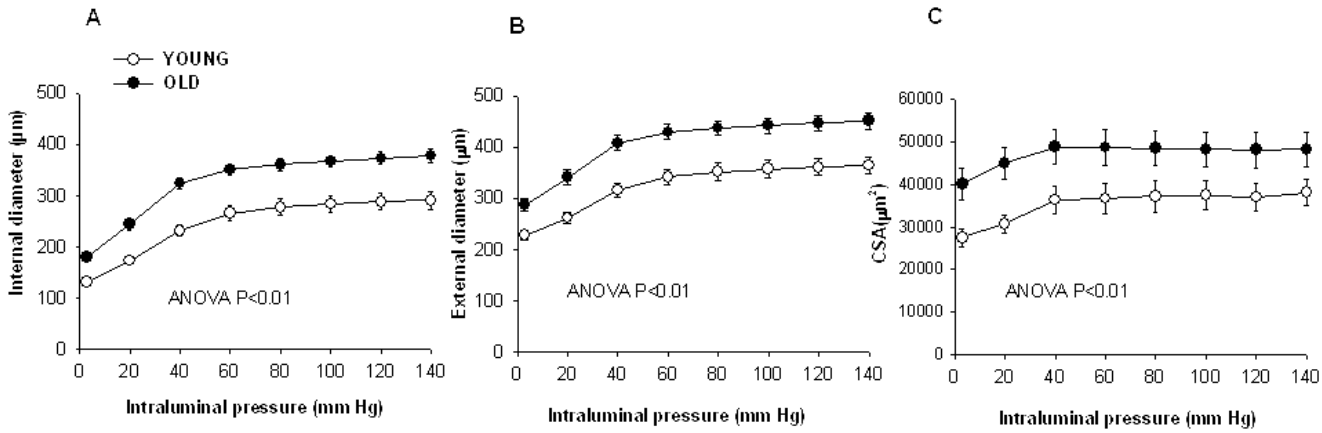

Figure 1. Internal diameter–intraluminal pressure (**A**), external diameter–intraluminal pressure (**B**), and cross-sectional area–intraluminal pressure (CSA) (**C**) in mesenteric resistance arteries from young and old rats incubated in calcium-free Krebs–Henseleit solution ($0Ca^{2+}$-KHS; omitting calcium and adding 10 mM EGTA). Data are expressed as means ± standard errors. $n = 7$ for each group. ANOVA, analysis of variance.

old rats. As a consequence, density of EC in the image area decreased with age (Table 1).

Results of SMC and EC nuclei morphology are shown in Figure 4. Total area of SMC nuclei was slightly greater in old than in young rats (Figure 4), indicating some hypertrophy of SMC from old animals. Similarly, total area of EC nuclei was greater in old than in young rats (Figure 4). The observed increase in total area was due to a greater nuclei length and width (Figure 4).

Collagen and Elastin Distribution

Figure 5 shows collagen distribution in MRA from young and old rats. Total collagen was greater in old than in young rats (young: 15.1 ± 3.9; old: 31.7 ± 1.3 arbitrary units; $p < .05$) (Figure 5A). Immunofluorescence experiments showed increased collagen I/III deposition in the media of old compared to young rats (Figure 5B).

Maximal projections of the IEL from both age groups are displayed in Figure 5C. Elastin is located in an external elastic lamina formed by isolated elastic fibers in a network (data not shown) and in a compact fenestrated IEL (Figure 5C) separating endothelium from media layers. IEL thickness and total fenestrae number were similar in both groups (Table 2). However, the mean fenestrae area was significantly greater in aged rats. Thus, the total volume of the IEL (elastin plus fenestrae) was greater in the old rats. However, the volume occupied by elastin within IEL was similar in both age groups (Table 2). Average fluorescence intensity per pixel was not significantly different between young and old rats, indicating no evidence for a difference in the total amount of elastin in a 1 mm length of artery (Table 2).

Discussion

MRAs from old rats showed hypertrophic outward remodeling, characterized by increased lumen and vessel diameter and CSA. This finding is in accordance with those from previous reports on the same arteries (6,7,9). The mechanisms underlying this process seem to involve different alterations in the wall of resistance arteries. Here we demonstrate that the increased WT is coupled to a greater media but unchanged adventitia thickness. The thickened media is not due to an increase of SMC number, because this remains unchanged with age, but can be related to alterations in cell size. Morphology of complete cells is very difficult to quantify within a whole intact artery because they make too many contacts with each other (18). There is evidence that SMC nuclear size correlates with SMC length (19). Therefore, we quantified SMC nuclei morphology clearly differentiated by their shape and orientation. In vessels from old rats, we observed some hypertrophy of SMC, as suggested by their larger nuclei size. In agreement, previous reports demonstrated hypertrophy of SMC from aged rat aorta (10). Our findings indicate that the same number of hypertrophied SMC reorganizes in a greater number of SMC layers in resistance arteries from old rats.

The adventitia, traditionally considered a structural support for the blood vessel, is emerging as an important player in the pathogenesis of cardiovascular diseases (18). Thus, some rat models of hypertension show an increased number of adventitial cells (20,21). Moreover, adventitial cells participate in collagen synthesis whereas elastin is mainly produced by SMC (22). Adventitial cell number was increased in resistance vessels from aged rats. This increase in adventitial cells is an unknown alteration in vessels from old individuals. It is therefore possible that adventitial cells are drivers of remodeling and may initiate other changes such as alterations in arrangement of SMC and in ECM production (18).

Endothelium is an important determinant in vivo of the lumen dimensions and overall vessel structure. In addition, the endothelium is in contact with circulating substances, including mitogens, and therefore the endothelium may be the first to undergo structural changes in abnormal situations. Aging is associated with a thickened intima or altered size of ECs (23). Here we found that ECs were also hypertrophied as shown by the increased nuclei area. This finding correlates with those of a previous report on tail artery from old rats (24). Observations obtained from both in vivo and in vitro experiments indicate that increased pulse pressure affects

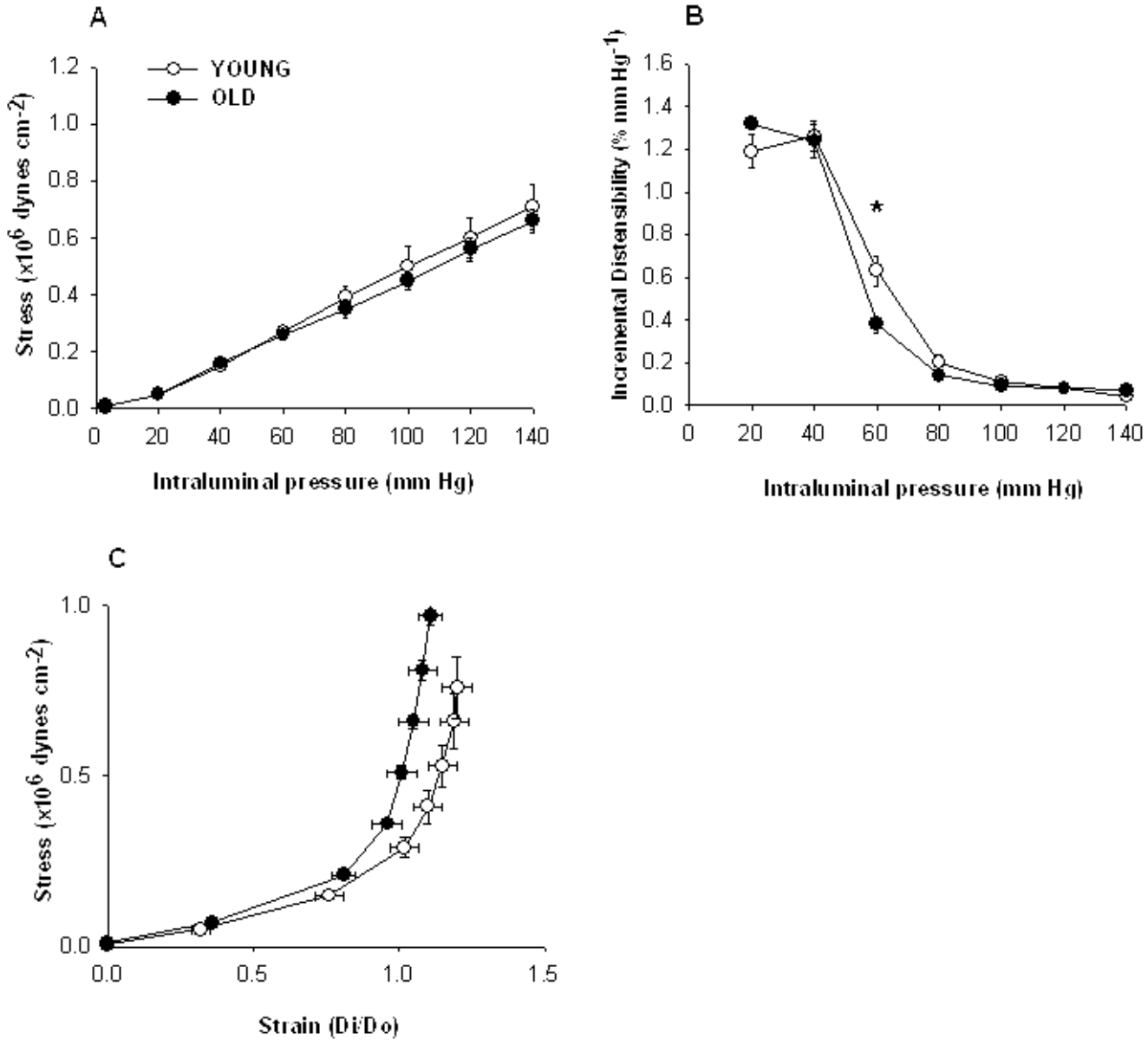

Figure 2. Stress–intraluminal pressure (**A**), incremental distensibility–intraluminal pressure (**B**), and stress–strain curves (**C**) in mesenteric resistance arteries from young and old rats incubated in calcium-free Krebs–Henseleit solution ($0Ca^{2+}$-KHS; omitting calcium and adding 10 mM EGTA). Data are expressed as means ± standard errors. $n = 7$ for each group.

endothelial integrity (25). It is therefore possible that the increased pulse pressure observed in old rats might participate in the altered EC morphology. ECs and SMC are interconnected by myoendothelial junctions, and endothelial factors are known to have trophic effects on the underlying cells. As ECs are greater in size, it is not surprising that SMC present the same phenotypic alteration. This phenotypic alteration might contribute to the overall hypertrophy of the vascular wall in resistance arteries from aged rats.

Changes in large arteries are well recognized with arterial distensibility showing an inverse association with age. It is interesting that this arterial ''stiffening'' seems to be largely confined to elastic arteries, with the most pronounced changes seen in the aorta (26–28). However, it becomes more and more evident that, as a result of increased pulse pressure owing to increased rigidity of large vascular conduits, both resistance arteries and capillary networks are also affected. Thus, resistance arteries from old rats also showed increased stiffness as shown by the greater β value (measure of intrinsic stiffness independent of geometry) and the leftward shift of the stress–strain relationship. There was no change in incremental distensibility of pressurized arteries except at 60 mmHg, where distensibility was found to be lower in old rats. Our findings indicate a moderate loss of vascular distensibility in resistance arteries from aged individuals. However, despite significant stiffening of wall

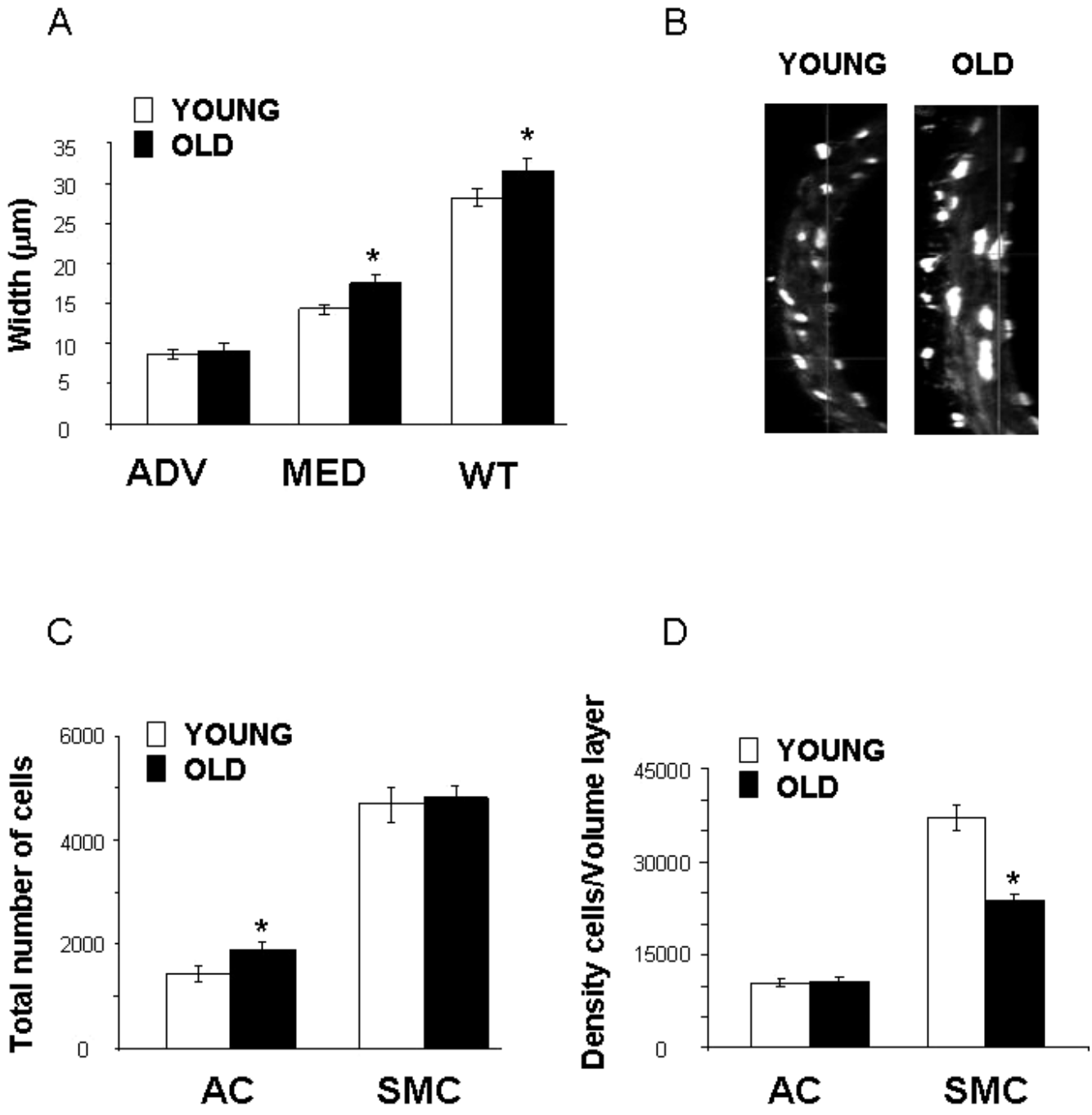

Figure 3. **A,** Effect of aging on width of adventitial (ADV) and media (MED) layers and on total wall thickness (WT) in mesenteric resistance arteries. **B,** Orthogonal sections obtained from confocal images of the vascular wall of mesenteric resistance arteries from young and old rats. **C** and **D,** Total number and density of adventitial (AC) and smooth muscle cells (SMC) of mesenteric resistance arteries from young and old rats. Arteries were incubated with Hoechst 33342 at 0.01 mg/mL to stain cell nuclei. Images were taken from slide-mounted vessels with an ×63 oil objective, zoom × 1 with a laser scanning confocal microscope. $n = 7$ for each group.

components, geometric adaptation has occurred to maintain normal in vivo wall stress, protecting the vessel wall from pressure-induced damage in vessels from old rats. This finding is in agreement with results recently published on the same vessels (7,9).

Age-related decreased elasticity seems to be the result of fragmentation, longitudinal fissures, and transverse breaks of elastic filaments (4,29,30). Therefore, the age-related modifications extensively described in the elastic fibers of all organs and tissues may be largely interpreted as result of progressive degradation of a protein polymer that has been produced early in life. In MRA, total elastin content did not differ among groups. However, the structure of IEL was qualitatively different, with the size of the fenestra being

significantly greater in arteries from old than from young rats. This alteration could be explained by diminished elastin cross-links (31), by an imbalance between elastin synthesis and degradation in favor of increased elastase activity, or by both. We have recently demonstrated that elastin digestion with elastase significantly enlarged fenestrae size in the IEL (32). Moreover, it is generally accepted that matrix metalloproteinase 2 (MMP2; a gelatinase that exhibits elastase activity) and proteins with elastase-type endopeptidase activities increase with age (30,33,34). Thus, it is highly possible that the increased fenestra area in the IEL from aged resistance arteries is associated with the higher elastolytic activity in aged rats. Moreover, it is known that, in the IEL, fenestrae enlarge along with artery development by fusion of neighboring fenestrae (35). Our results suggest that this enlargement of fenestra size would last until late stages of life.

Aging modulates the vascular SMC phenotype towards the synthetic state, which might participate in the increase in ECM protein synthesis (36). Stiffening of elastic arteries is related, among other things, to degenerative changes in the structure of elastin. However, the amount and type of collagen is also important. Collagen is increased in large arteries from both aged animals and humans (3,4,37). In resistance arteries from young rats, collagen was distributed along the whole vascular wall, with higher deposition in the adventitial layer. In vessels from old rats, collagen deposition increased in the media layer. Among the 26 different collagen types described until now, type I and III are the major fibrillar collagens detectable in vessels, representing 60% and 30% of vascular collagens, respectively (3,4). Herein, we show increased collagen I/III deposition in the media layer from old compared to young rats. Because the total amount of elastin did not change and collagen increased in vessels from aged rats, the gradual shift from elastin- to collagen-dominant state, together with alterations in the three-dimensional structure of elastin, is a possible cause of the loss of elasticity and the gain of stiffness in the aging resistance vessels.

Changes in vascular morphology can be related to body weight. However, age-related morphological changes can also be a consequence of changes in blood pressure. Systolic and diastolic blood pressures were similar but pulse pressure was increased in old compared to young rats. These findings are consistent with those observed by other authors both in rats and in humans (6–8,24,38). There is increasing evidence suggesting a relationship between pulse pressure and vascular structure in resistance arteries (6,7). In this sense, pulsatile stretch has been shown to promote vascular hypertrophy by increasing vascular SMC proliferation and matrix synthesis (39,40). Moreover, mechanical strain induces human vascular matrix synthesis through angiotensin II–dependent mechanisms (41). Therefore, we cannot exclude that, in addition to the aging process, the fibrotic changes observed in mesenteric arteries from old rats are linked, at least partially, to elevated pulse pressure. In fact, in the Framingham Heart Study cohort, Mitchell and colleagues (42) suggested that increased forward transmission of a larger forward wave in aged individuals may expose the peripheral small arteries and microvessels to damaging levels of pressure pulsatility and may contribute to an emerging spectrum of microvascular disorders that are common in the elderly population.

Table 1. Laser Scanning Confocal Microscope Measurements of Endothelial Cell Layer in Mesenteric Arteries From Young and Old Rats

EC Layer Measurements	Young	Old
LSA (μm^2)	0.793 ± 0.04	1.08 ± 0.04*
Density EC (EC/mm^2)	1905 ± 39	1558 ± 44*
Total number EC	1510 ± 67	1649 ± 44

Notes: Data are expressed as mean ± standard error of the mean ($n = 7$ animals).

*$p < .05$ vs young rats.

LSA = luminal surface area; EC = endothelial cells.

Summary

The present study demonstrates that the increased thickness of the vascular wall of resistance arteries from aged rats is mainly due to greater media thickness. The same number of hypertrophied SMC reorganizes in a greater number of SMC layers leading to a thickened media. Moreover, the number of adventitial cells and the size of endothelial nuclei increased with age. We also observed an increase in collagen I/III in the media. This finding suggests that fibrosis might occupy cellular gaps left between vascular SMC, also contributing to the thickened media. This fibrotic process, together with changes in elastin structure, might be responsible for the increased stiffness of resistance arteries from aged rats.

Limitations and Future Perspectives

The small mesenteric arteries have been extensively used to study the implications of altered vascular structure and mechanics in age-related cardiovascular diseases such as hypertension. However, taking into account the reported heterogeneity of the aged cardiovascular system, specific studies aimed to analyze the structural and mechanical alterations of other resistance vascular beds (i.e., coronary microvessels and/or cerebral vessels) seem necessary. The knowledge of these alterations and their associated mechanisms would add important insights into age-related vascular alterations. More importantly, despite the fact that several studies have analyzed the contribution of structural alterations of resistance arteries to human hypertension (43–45), very little is known of the impact of the aging process on human small arteries.

To our knowledge, there are no studies analyzing the impact of structural and mechanical changes of resistance arteries on age-associated cardiovascular risk. However, structural alterations of small artery walls are the most potent predictors of cardiovascular events in a selected high-risk population (43). It is well known that small artery remodeling may lead to complications of cardiovascular diseases including myocardial ischemia, stroke, and renal failure. It is therefore possible that these structural alterations of small vessels might contribute to deleterious consequences of aging on target organs. Knowledge of these alterations and their underlying mechanisms seems of particular

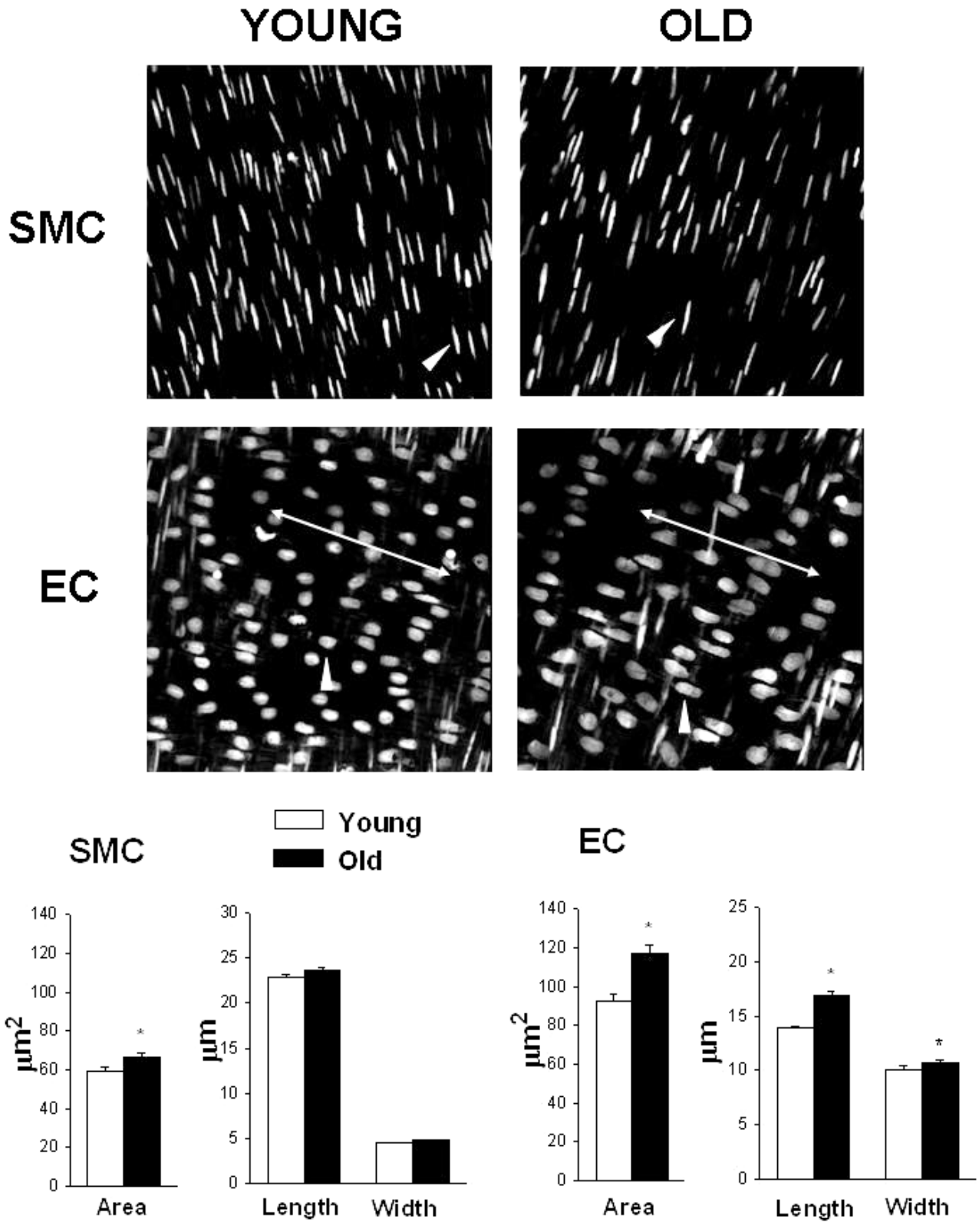

Figure 4. Representative microphotographs of laser scanning confocal microscopy images of nuclei from smooth muscle cells (SMC) and endothelial cells (EC) from mesenteric resistance arteries from young and old rats (*top*). Comparison of morphological parameters of SMC and EC nuclei from images of pressure-fixed mesenteric resistance arteries from young and old rats (*bottom*). Arteries were incubated with propidium iodide 10 mg/mL to stain cell nuclei. The images were taken from slide-mounted vessels with a ×63 oil objective, zoom × 1 with a laser scanning confocal microscope. *Lines with arrows* show the longitudinal axis of the vessel. *Arrowheads* point to representative nuclei. Image dimensions: 238 × 238 μm. $n = 7$ for each group.

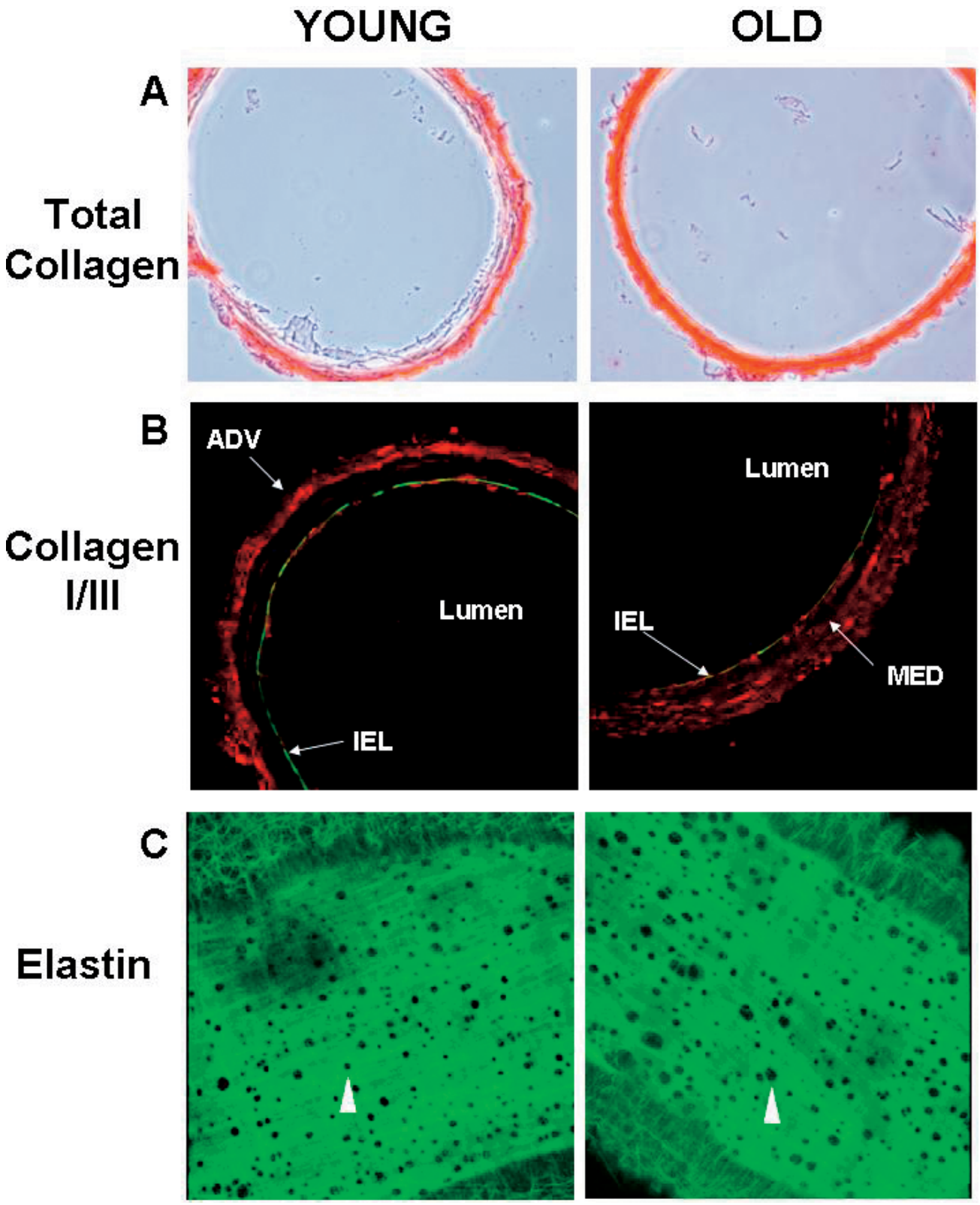

Figure 5. **A,** Representative images (from five animals) of collagen staining with picrosirius red of transversal sections obtained from mesenteric resistance arteries from young and old rats. Images were captured with a light microscope (×40 objective, zoom × 1). Image size: 325 × 325 μm. **B,** Representative photomicrographs (from four animals) of collagen I/III immunofluorescence in mesenteric resistance arteries from young and old rats. Collagen I/III was labeled with a secondary antibody conjugated to Alexa 594 (*red*). Natural autofluorescence of elastin was used to delimitate intima and media layers (*green*). ADV, adventitia layer; MED, media layers. Image size: 256 × 256 μm. **C,** Confocal projections of the internal elastic lamina of mesenteric resistance arteries from young and old rats. Vessels were pressure-fixed at 70 mmHg and mounted intact on a slide. Projections were obtained from serial optical sections captured with a fluorescence confocal microscope (×40 oil immersion objective, zoom × 1). Image size: 256 × 256 μm. *Arrowheads* indicate localization of one fenestra. $n = 7$ for each group.

Table 2. Characteristics of Internal Elastic Lamina in Pressurized Segments of Mesenteric Resistance Arteries From Young and Old Rats

IEL Characteristics	Young	Old
Thickness, μm	3.6 ± 0.13	3.3 ± 0.1
Total no. of fenestrae	6388 ± 741	5349 ± 425
Fenestra area, μm^2	13.3 ± 0.83	19.5 ± 1.1*
Volume/artery, mm^3	0.0029 ± 0.0002	0.0035 ± 0.0002†
Volume of elastin/artery, mm^3	0.0025 ± 0.0002	0.0029 ± 0.0001
Intensity/pixel	23.7 ± 1.51	25.2 ± 3.1
Total fluorescence, $\times 10^6$ (intensity/pixel × volume)	692 ± 57	899 ± 129

Notes: Data are expressed as mean ± standard error of the mean ($n = 7$ animals).

*$p < .01$ vs young rats.

†$p < .05$ vs young rats.

IEL = internal elastic lamina.

importance to assess their contribution in age-associated cardiovascular damage. As suggested, interactions between macro- and microcirculation may affect pulsatile forces acting on large and small arteries all the way to microvessels resulting in increased cardiovascular risk (46).

Acknowledgments

This study was supported by grants from Dirección General de Ciencia y Tecnologia (SAF 2003-1001), Fondo de Investigaciones Sanitarias (04/1295), and Generalitat de Catalunya (2005SGR80). A.M.B. was partially supported by Dirección General de Universidades e Investigación (Consejería de Educación de la Comunidad de Madrid (02/0372/2002).

We acknowledge the technical assistance of the Servei de Microscopia from the Universitat Autònoma de Barcelona.

Part of this work was presented at the 8th International Symposium on Resistance Arteries, Angers, France, June 20–23, 2004.

Ana M. Briones is currently with the Departamento de Farmacología y Terapéutica, Facultad de Medicina, Universidad Autónoma de Madrid, Spain.

Correspondence

Address correspondence to Elisabet Vila, PhD, Departament de Farmacologia, Terapèutica i Toxicología, Facultat de Medicina, Universitat Autònoma de Barcelona, Bellaterra, 08193 Barcelona (Spain). E-mail: elisabet.vila@uab.es

References

1. Folkow B, Svanborg A. Physiology of cardiovascular aging. *Physiol Rev*. 1993;73:725–764.
2. Marín J, Rodríguez-Martínez MA. Age-related changes in vascular responses. *Exp Gerontol*. 1999;34:503–512.
3. Jacob MP. Extracellular matrix remodeling and matrix metalloproteinases in the vascular wall during aging and in pathological conditions. *Biomed Pharmacother*. 2003;57:195–202.
4. Dao HH, Essalihi R, Bouvet C, Moreau P. Evolution and modulation of age-related medial elastocalcinosis: impact on large artery stiffness and isolated systolic hypertension. *Cardiovasc Res*. 2005;66:307–317.
5. Hajdu MA, Heistad DD, Siems JE, Baumbach GL. Effects of aging on mechanics and composition of cerebral arterioles in rats. *Circ Res*. 1990;66:1747–1754.
6. Moreau P, d'Uscio LV, Luscher TF. Structure and reactivity of small arteries in aging. *Cardiovasc Res*. 1998;37:247–253.
7. Laurant P, Adrian M, Berthelot A. Effect of age on mechanical properties of rat mesenteric small arteries. *Can J Physiol Pharmacol*. 2004;82:269–275.
8. Benetos A, Waeber B, Izzo J, et al. Influence of age, risk factors, and cardiovascular and renal disease on arterial stiffness: clinical applications. *Am J Hypertens*. 2002;15:1101–1108.
9. Adrian M, Laurant P, Berthelot A. Effect of magnesium on mechanical properties of pressurized mesenteric small arteries from old and adult rats. *Clin Exp Pharmacol Physiol*. 2004;31:306–313.
10. Cliff WJ. The aortic tunica media in aging rats. *Exp Mol Pathol*. 1970;13:172–189.
11. Orlandi A, Mauriello A, Marino B, Spagnoli LG. Age-related modifications of aorta and coronaries in the rabbit: a morphological and morphometrical assessment. *Arch Gerontol Geriatr*. 1993;17:37–53.
12. Corman B, Duriez M, Poitevin P, et al. Aminoguanidine prevents age-related arterial stiffening and cardiac hypertrophy. *Proc Natl Acad Sci U S A*. 1998;95:1301–1306.
13. Marín J. Age-related changes in vascular responses: a review. *Mech Ageing Dev*. 1995;79:71–114.
14. Briones AM, González JM, Somoza B, et al. Role of elastin in spontaneously hypertensive rat small mesenteric artery remodelling. *J Physiol*. 2003;552:185–195.
15. Arribas SM, Hillier C, González C, McGrory S, Dominiczak AF, McGrath JC. Cellular aspects of vascular remodeling in hypertension revealed by confocal microscopy. *Hypertension*. 1997;30:1455–1464.
16. Blomfield J, Farrar JF. The fluorescent properties of maturing arterial elastin. *Cardiovasc Res*. 1969;3:161–170.
17. Briones AM, Xavier FE, Arribas SM, et al. Alterations in structure and mechanics of resistance arteries from ouabain induced hypertensive rats. *Am J Physiol Heart Circ Physiol*. 2006;291:H193–H201.
18. McGrath JC, Deighan C, Briones AM, et al. New aspects of vascular remodelling: the involvement of all vascular cell types. *Exp Physiol*. 2005;90:469–475.
19. Dickhout JG, Lee RMKW. Increased medial smooth muscle cell length is responsible for vascular hypertrophy in young hypertensive rats. *Am J Physiol Heart Circ Physiol*. 2000;279:H2085–H2094.
20. Arribas SM, González C, Graham D, Dominiczak AF, McGrath JC. Cellular changes induced by chronic nitric oxide inhibition in intact rat basilar arteries revealed by confocal microscopy. *J Hypertens*. 1997;15:1685–1693.
21. Kantachuvesiri S, Fleming S, Peters J, et al. Controlled hypertension, a transgenic toggle switch reveals differential mechanisms underlying vascular disease. *J Biol Chem*. 2001;276:36727–36733.
22. Ruckman JL, Luvalle PA, Hill KE, Giro MG, Davidson JM. Phenotypic stability and variation in cells of the porcine aorta: collagen and elastin production. *Matrix Biol*. 1994;14:135–145.
23. Haudenschild CC, Prescott MF, Chobanian AV. Aortic endothelial and subendothelial cells in experimental hypertension and aging. *Hypertension*. 1981;3:I148–I153.
24. Vila E, Vivas NM, Tabernero A, Giraldo J, Arribas SM. Alpha 1-adrenoceptor vasoconstriction in the tail artery during ageing. *Br J Pharmacol*. 1997;121:1017–1023.
25. Davies PF. Flow-mediated endothelial mechanotransduction. *Physiol Rev*. 1995;75:519–560.
26. Chowienczyk P. Vascular ageing. *Clin Sci (Lond)*. 2002;102:601–602.
27. Lakatta EG. Arterial and cardiac aging: major shareholders in cardiovascular disease enterprises: Part III: cellular and molecular clues to heart and arterial aging. *Circulation*. 2003;107:490–497.
28. Safar ME. Peripheral pulse pressure, large arteries, and microvessels. *Hypertension*. 2004;44:121–122.
29. Pasquali-Ronchetti I, Baccarani-Contri M. Elastic fiber during development and aging. *Microsc Res Tech*. 1997;38:428–435.
30. Li Z, Froehlich J, Galis ZS, Lakatta EG. Increased expression of matrix metalloproteinase-2 in the thickened intima of aged rats. *Hypertension*. 1999;33:116–123.
31. Watanabe M, Sawai T, Nagura H, Suyama K. Age-related alteration of cross-linking amino acids of elastin in human aorta. *Tohoku J Exp Med*. 1996;180:115–130.
32. González JM, Briones AM, Somoza B, et al. Postnatal alterations in elastic fiber organization precede resistance artery narrowing in SHR. *Am J Physiol Heart Circ Physiol*. 2006;291:H804–H812.
33. Robert L. Elastin, past, present and future. *Pathol Biol (Paris)*. 2002;50:503–511.
34. Wang M, Takagi G, Asai K, et al. Aging increases aortic MMP-2 activity and angiotensin II in nonhuman primates. *Hypertension*. 2003;41:1308–1316.

35. Wong LC, Langille BL. Developmental remodeling of the internal elastic lamina of rabbit arteries: effect of blood flow. *Circ Res.* 1996; 78:799–805.
36. Orlandi A, Bochaton-Piallat ML, Gabbiani G, Spagnoli LG. Aging, smooth muscle cells and vascular pathobiology: implications for atherosclerosis. *Atherosclerosis.* 2006;188:221–230.
37. London GM, Marchais SJ, Guerin AP, Pannier B. Arterial stiffness: pathophysiology and clinical impact. *Clin Exp Hypertens.* 2004;26: 689–699.
38. Arribas SM, Vila E, McGrath JC. Impairment of vasodilator function in basilar arteries from aged rats. *Stroke.* 1997;28:1812–1820.
39. Owens GK. Role of mechanical strain in regulation of differentiation of vascular smooth muscle cells. *Circ Res.* 1996;79:1054–1055.
40. O'Callaghan CJ, Williams B. Mechanical strain-induced extracellular matrix production by human vascular smooth muscle cells: role of TGF-beta(1). *Hypertension.* 2000;36:319–324.
41. Stanley AG, Patel H, Knight AL, Williams B. Mechanical strain-induced human vascular matrix synthesis: the role of angiotensin II. *J Renin Angiotensin Aldosterone Syst.* 2000;1:32–35.
42. Mitchell GF, Parise H, Benjamin EJ, et al. Changes in arterial stiffness and wave reflection with advancing age in healthy men and women: the Framingham Heart Study. *Hypertension.* 2004;43:1239–1245.
43. Rizzoni D, Porteri E, Boari GE, et al. Prognostic significance of small-artery structure in hypertension. *Circulation.* 2003;108:2230–2235.
44. Schiffrin EL, Touyz RM. From bedside to bench to bedside: role of renin-angiotensin-aldosterone system in remodeling of resistance arteries in hypertension. *Am J Physiol Heart Circ Physiol.* 2004;287: H435–H446.
45. Mulvany MJ. Abnormalities of the resistance vasculature in hypertension: correction by vasodilator therapy. *Pharmacol Rep.* 2005;57Suppl: 144–150.
46. Safar ME. Peripheral pulse pressure, large arteries and microvessels. *Hypertension.* 2004;44:121–122.

Received July 27, 2006
Accepted February 15, 2007
Decision Editor: Huber R. Warner, PhD